

Molecular structure of the sarcomeric Z-disk: two types of titin interactions lead to an asymmetrical sorting of α -actinin

Paul Young, Charles Ferguson,
Sonia Bañuelos and Mathias Gautel¹

European Molecular Biology Laboratory, Postfach 10 22 09,
69012 Heidelberg, Germany

¹Corresponding author
e-mail: gautel@embl-heidelberg.de

The sarcomeric Z-disk, the anchoring plane of thin (actin) filaments, links titin (also called connectin) and actin filaments from opposing sarcomere halves in a lattice connected by α -actinin. We demonstrate by protein interaction analysis that two types of titin interactions are involved in the assembly of α -actinin into the Z-disk. Titin interacts via a single binding site with the two central spectrin-like repeats of the outermost pair of α -actinin molecules. In the central Z-disk, titin can interact with multiple α -actinin molecules via their C-terminal domains. These interactions allow the assembly of a ternary complex of titin, actin and α -actinin *in vitro*, and are expected to constrain the path of titin in the Z-disk. In thick skeletal muscle Z-disks, titin filaments cross over the Z-disk centre by ~30 nm, suggesting that their α -actinin-binding sites overlap in an antiparallel fashion. The combination of our biochemical and ultrastructural data now allows a molecular model of the sarcomeric Z-disk, where overlapping titin filaments and their interactions with the α -actinin rod and C-terminal domain can account for the essential ultrastructural features.

Keywords: α -actinin/connectin/muscle structure/nebulin/titin

Introduction

Cells exert their mechanical functions, both actively and passively, by specialized structures of their cytoskeleton. In this intracellular scaffold, filamentous systems of intermediate filaments, microtubules or actin stress fibres dissipate mechanical strain and maintain cell shape. Of particular importance is the organization of the actin cytoskeleton in muscle cells, where a stable anchorage of actin filaments at the plasma membrane and at the Z-disk of the sarcomere is required for the transmission of mechanical strain along the serially arranged sarcomeres, and ultimately along the length of the muscle. Actin filaments from adjacent sarcomeres are anchored in the Z-disk of striated muscles. Each actin filament overlaps with four filaments from the opposite sarcomere, forming a square lattice which is cross-connected in a zig-zag pattern by Z-filaments, assumed to consist of α -actinin (see Luther, 1991, and references therein). The periodicity of α -actinin in this lattice has been measured as between

15 and 20 nm in native Z-disks (Luther, 1991; Schroeter *et al.*, 1996). The number of α -actinin cross-links and hence the thickness of Z-disks is greatly variable, presumably to adapt the Z-disk structure to the level of mechanical strain (Vigoreaux, 1994). Within a given muscle fibre, however, their number is tightly regulated (reviewed in Squire, 1981). The sarcomeric Z-disk therefore represents a model system for the controlled assembly of actin filaments.

How is this variability in Z-disk assembly controlled? A ruler-like protein, containing variable numbers of specific binding sites for other Z-disk components, could control the number of α -actinin molecules and their spacing. In muscle, two giant proteins, titin and the actin-binding nebulin, are possible candidates to act as a molecular blueprint (see review by Trinick, 1994). Titin (Wang *et al.*, 1979; described as connectin by Maruyama *et al.*, 1977) is believed to function as the organizer of the sarcomere by providing specific, spatially defined binding sites for other sarcomeric proteins over the entire distance from Z-disk to M-band (see reviews by Trinick, 1994, 1996; Maruyama, 1997). Titin appears as one of the first sarcomeric proteins during myofibrillogenesis, and is detected in dot-like aggregates which co-localize with α -actinin (Tokuyasu and Maher, 1987; Fürst *et al.*, 1989) in differentiating myoblasts. These dots align on actin stress fibres and are organized into Z-disks during the progression of myofibrillogenesis (Dlugosz *et al.*, 1984; Dabiri *et al.*, 1997). The titin molecule is constructed in a modular fashion from ~280 immunoglobulin- and fibronectin-3-like domains and specific sequences in the Z-disk, I-band and M-band (Labeit and Kolmerer, 1995a). Only a small region of titin, between 60 and 120 kDa of the ~3 MDa protein, is localized within the Z-disk (Gautel *et al.*, 1996; Yajima *et al.*, 1996). This central Z-disk region contains four immunoglobulin-like domains (Labeit and Kolmerer, 1995a), several phosphorylation sites and a variable number of copies of a specific protein motif, the 45 residue Z-repeat (Gautel *et al.*, 1996) (Figure 1A). It is now evident that the Z-repeats are differentially spliced in the central Z-disk region of titin (Gautel *et al.*, 1996; Sorimachi *et al.*, 1997), and that their number correlates closely to the thickness of Z-disks in the respective muscle type (Ohtsuka *et al.*, 1997a; Peckham *et al.*, 1997). The simple zig-zag Z-disk of avian fast muscle contains only two Z-repeats (Ohtsuka *et al.*, 1997a), whereas mammalian Z-disks with two or more Z-filaments (Rowe, 1973) contain four or more titin Z-repeats (Gautel *et al.*, 1996; Peckham *et al.*, 1997; Sorimachi *et al.*, 1997). Similarly, the actin-binding repeats of nebulin are proposed to span the Z-disk (Labeit and Kolmerer, 1995b) where adult and fetal isoforms show different numbers of a special repeat (Labeit and Kolmerer, 1995b; Wang *et al.*, 1996).

If titin were indeed to act as a ruler for Z-disk assembly,

the central Z-disk region of the molecule should contain binding sites for other sarcomeric proteins. In agreement with this, native titin binds to α -actinin *in vitro* (Jeng and Wang, 1992). More specifically, recombinant fragments of Z-disk titin bind to α -actinin (Turnacioglu *et al.*, 1996; Ohtsuka *et al.*, 1997b). Genetic interaction screens have identified a binding site for titin in the C-terminal domain of α -actinin [homologous to calmodulin (CaM) but containing a non-functional EF hand], and localized this interaction to a subset of the titin Z-repeats (Ohtsuka *et al.*, 1997a; Sorimachi *et al.*, 1997). Titin Z-repeats form two subgroups, the two invariant flanking repeats being most closely related to each other, whereas the differentially spliced central repeats form a distinct subgroup (Gautel *et al.*, 1996). The interaction studies in yeast two-hybrid assays suggested that only the flanking type of repeats bind to α -actinin, whereas the central type of repeats do not interact (Ohtsuka *et al.*, 1997a). It is as yet unclear how the binding sites on titin and the ultrastructural layout of the molecules are correlated. In thin Z-disks with a single Z-filament in projection, like chicken *M. pectoralis major* (Fürst *et al.*, 1988; Yajima *et al.*, 1996), the N-terminal region of titin cannot be resolved within the Z-disk centre by immunoelectron microscopy. Our own

studies in thick cardiac Z-disks suggested a central position for the N-terminal region with little or no overlap of titin (Gautel *et al.*, 1996). However, if titin were to control the number of Z-filaments, one would expect some degree of titin overlap in the Z-disk reflecting the degree of thin filament overlap. The understanding of the molecular layout in the central Z-disk requires, therefore, a more highly resolved definition of the position of the titin N-terminus.

Further important questions arise about the exact nature of the sorting mechanisms of α -actinin. Transfection experiments in myogenic cells have demonstrated that α -actinin, lacking the C-terminal domain, is also sorted to the sarcomeric Z-disk (Schultheiss *et al.*, 1992). This α -actinin causes Z-disk misassembly during the progression of myofibrillogenesis and the formation of Z-rods reminiscent of those formed in nemaline myopathy (Schultheiss *et al.*, 1992). The binding of titin to the C-terminal domain of α -actinin therefore appears not to be the sole protein interaction that controls the sarcomeric sorting of the molecule. Rather, a second Z-disk-specific binding site could be predicted from these observations, which should be important for the correct assembly of the Z-disk.

In this work, we have identified this second sarcomeric binding site of α -actinin as an interaction between the spectrin-like repeats (slrs) and a single site on titin. We also demonstrate that the central Z-repeats of titin can interact equally with the C-terminal domain of α -actinin, similarly to the flanking repeats. These interactions control the assembly of ternary complexes of titin, α -actinin and actin *in vitro*. We combine these biochemical observations with refined ultrastructural data on the position of the N-terminus of titin and the C-terminus of nebulin, and can now propose a molecular model of titin, actin and α -actinin in the sarcomeric Z-disk.

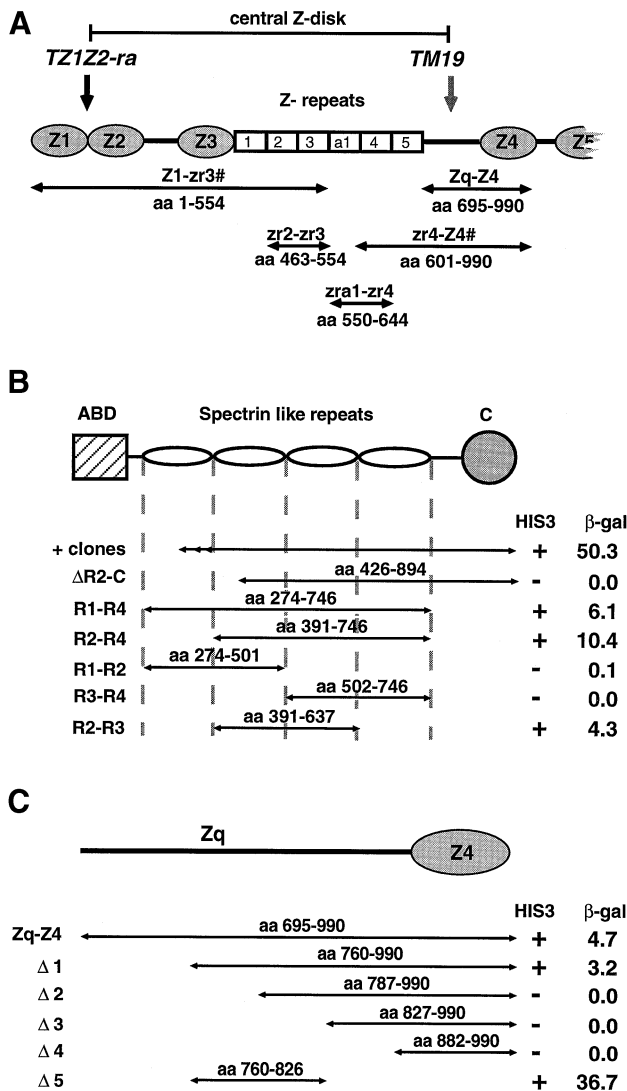


Fig. 1. (A) Domain pattern and positions of ultrastructurally defined epitopes in the Z-disk region of titin. Only four of >200 titin immunoglobulin domains are shown. TZ1Z2-ra is the position of our new polyclonal antibody. The position of the previously mapped TM19 (Gautel *et al.*, 1996) is also shown. The ultrastructurally defined central Z-disk region is marked. The primary bait constructs used in this study are shown as bars. Baits interacting with the α -actinin C-terminal domain are marked with #. Ig domains are shown as ovals, Z-repeats as squares. The numbering of the modules is as in Labeit and Kolmerer (1995a) and Gautel *et al.* (1996). Non-modular sequences are shown as lines. (B) The extent of α -actinin clones obtained in the Zq-Z4 two-hybrid screen (+ clones) and the subfragments used to map the titin-binding site on α -actinin. Note that the spectrin-like repeats 2 and 3 are both necessary and sufficient to interact with titin. Δ R2-C corresponds to the longest clone obtained in the screen by Ohtsuka *et al.* (1997b); this clone interacts with baits containing Z-repeats zr1 or zr5 but not with Zq-Z4. ABD, actin-binding domain; C, C-terminal domain. The residues in the α -actinin 2A isoform are given above each construct. (C) The interaction of α -actinin and titin was mapped on titin by successive deletions of the Zq-Z4 bait. Interaction of the deletion constructs with the smallest α -actinin-fragment R2-R3 shown to interact above was tested in the two-hybrid system. The deletion clones Δ 2- Δ 4 are negative in this assay, and we conclude that the titin-binding site is localized in the cross-species conserved residues 760-826 of titin. The Ig domain Z4 (oval as in A) is not necessary for binding. The HIS3 reporter gene activation is marked as + or -; β -galactosidase gene activation is given in arbitrary units from liquid assays. Note that the two-hybrid system assays the interaction of fusion proteins as hybrid transcription factors and that the β -galactosidase units therefore reflect transcriptional activation and may not directly express the relative strength of the interactions.

Results

A single site on titin binds to the rod domain of α -actinin at the edge of the central Z-disk

In a systematic quest for ligands of titin in the region that we mapped to the central Z-disk at the ultrastructural level, we used several cDNA baits (summarized in Figure 1A) from that region to screen a skeletal muscle cDNA library in the two-hybrid system. Several of these baits were found to interact with α -actinin cDNAs. The bait Zq-Z4 contains the non-modular region C-terminal to the Z-repeats of titin and the immunoglobulin-like domain Z4 (amino acids 695–990 of titin), and is ultrastructurally located at the edge of the central Z-disk (Gautel *et al.*, 1996; Yajima *et al.*, 1996). The yeast two-hybrid screen with this region yielded >240 *HIS3*- and β -galactosidase-positive clones from $\sim 5 \times 10^5$ transformants. Library plasmids were rescued from 16 colonies, and the inserts from five were partially sequenced. All were found to contain cDNA fragments of the muscle α -actinin 2A isoform (Beggs *et al.*, 1992; DDBJ/EMBL/GenBank accession no. M86406). These clones are fused to the Gal4 activation domain in a very narrow region of amino acids 338–367 within helices B and C (Yan *et al.*, 1993) of the first slr of the rod domain (Figure 1). Restriction endonuclease analysis using the internal *Bgl*III restriction site (amino acid 421) near to the start of the second slr, and PCR analysis of the 11 remaining clones indicated that all α -actinin clones follow the same pattern.

Ohtsuka *et al.* (1997a,b) identified an interaction between chicken titin and α -actinin in a two-hybrid screen using a 63 kDa N-terminal fragment of avian titin as bait. Since the bait of Ohtsuka *et al.* overlaps with ours by ~ 100 amino acids, we wanted to establish if we had identified a distinct binding site. Therefore, an α -actinin construct corresponding to the largest interacting cDNA from their screen (Figure 1B) was cloned into pGAD-10 and found not to interact with our titin bait. To investigate further the exact site of interaction between titin and α -actinin, a series of deletion clones of α -actinin (Figure 1B) was assayed for titin interaction by co-transformation with the Zq-Z4 bait in L40 cells. Binding to titin Zq-Z4 is independent of the presence of the C-terminal domain of α -actinin. The smallest fragment that still interacts contains slrs 2 and 3 (Figure 1B). Of the remaining baits, those containing either the Z-repeats zr1 or zr5 interact with α -actinin clones containing the CaM-like C-terminal domain, confirming the earlier observations of Ohtsuka *et al.* (1997) and Sorimachi *et al.* (1997) (Figure 1A).

The novel α -actinin-binding site thus identified on titin was mapped down within the original bait by a series of smaller fragments depicted in Figure 1C. Their ability to interact with the α -actinin R2-R3 construct was determined in two-hybrid assays scoring the activation of the *HIS3* and β -galactosidase reporter genes. The smallest construct showing an interaction contains amino acids 760–826 of titin. The flanking sequences showed no interaction (Figure 1C).

Titin binds the two central repeats of the α -actinin rod in a tight complex

Since the two-hybrid system assays the interaction of fusion proteins as chimeric transcription factors, we con-

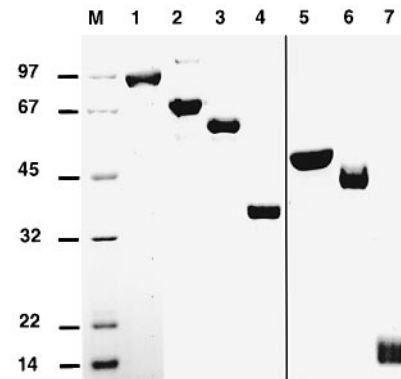


Fig. 2. Recombinant α -actinin (lanes 1–4) and titin fragments (lanes 5–7) used in this study. Proteins were purified as described in Materials and methods and analysed on 15% SDS-PAGE. The calculated molecular weights generally agree well with their electrophoretic mobility although the apparent molecular weight of some fragments is slightly higher. Lane 1, α -actinin 2A (mol. wt 104 kDa); lane 2, R1-C (74 kDa); lane 3, R1-R4 (57 kDa); lane 4, R2-R3 (30 kDa); lane 5, titin zr4-Z4 (44 kDa); lane 6, Zq-Z4 (33 kDa); lane 7, zr2-zr3 (11 kDa). M: marker lane, sizes in kDa.

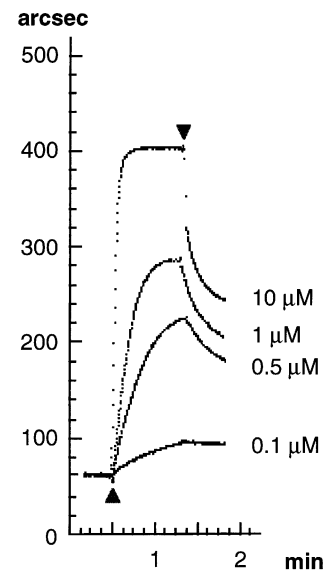


Fig. 3. Titin binds with high affinity to the α -actinin rod. Biosensor assay for the binding of titin Zq-Z4 to recombinant α -actinin R1-R4. The response in arcsec is shown for four different concentrations of the titin fragment. The beginning of association and dissociation phases are marked with triangles. Concentration-dependent binding with high affinity is observed. Analysis of triple experiments with the FastFit software (see Materials and methods) yielded an apparent K_d of 240 nM.

firmed the two-hybrid data by independent binding results. The Zq-Z4 bait fragment was expressed in *Escherichia coli* (Figure 2), encoding more than the minimal binding site defined above to ensure proper folding of the motif. The protein was assayed in a Biosensor (Davies and Pollard Knight, 1993) for binding to the α -actinin rod fragment R1-R4 (amino acids 274–746). Concentration-dependent binding of Zq-Z4 to R1-R4 (Figure 3) within a range of 100 nM to 50 μ M of ligand was observed. The apparent K_d of the interaction was calculated as described in Materials and methods and is ~ 240 nM. This confirms the two-hybrid data, and we conclude that titin binds with high affinity to the rod domain of α -actinin.

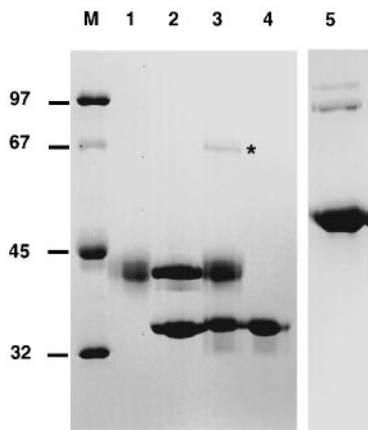


Fig. 4. Titin and the central spectrin like repeats of α -actinin can form a 1:1 complex. Chemical cross-linking demonstrates the formation of a 1:1 complex in the absence of dimerization of the R2–R3 fragment of α -actinin. Lane 1, titin Zq–Z4 cross-linked; lane 2, α -actinin R2–R3 and titin Zq–Z4 not cross-linked; lane 3, α -actinin R2–R3 and titin Zq–Z4 cross-linked; lane 4, α -actinin R2–R3 cross-linked; lane 5, α -actinin R1–R4 cross-linked in a separate experiment. Note the appearance of dimer and tetramer bands with R1–R4 in agreement with the data of Flood (1995). Cross-linking of α -actinin R2–R3 and titin Zq–Z4 results in an additional band of approximate mol. wt 66 kDa which is specific for the presence of both proteins (asterisk). M: marker lane, sizes in kDa.

As α -actinin forms an antiparallel dimer, this property raises the question of whether the interaction of titin within the central two slrs is dependent upon dimer formation. We therefore investigated the stoichiometry of the complex by chemical cross-linking. While the fragment R1–R4, comprising the entire rod domain, can be shown to dimerize under the conditions used, repeats R2–R3 cannot (Figure 4). Similarly, analytical gel filtration of R2–R3 shows a single peak consistent with a monomer (not shown). The titin fragment Zq–Z4 can be cross-linked to R2–R3, with the cross-linked product appearing at ~66 kDa, which is equivalent to the sum of the molecular weights of the two protein fragments (Figure 4). We conclude that the formation of a 1:1 complex in the absence of any detectable dimer formation of the central α -actinin rod fragment suggests that the interaction of titin and the rod domain is dimerization independent, and that the binding site is formed solely by the two slrs R2 and R3. Again, binding to the R2–R3 fragment confirms the results of the two-hybrid assays.

Central titin Z-repeats interact with the α -actinin C-terminal domain

In our two-hybrid assays, baits containing the flanking Z-repeats zr1 and zr5 interact with α -actinin in the presence of the C-terminal CaM-like domain (summarized in Figure 1A), consistent with earlier reports (Ohtsuka *et al.*, 1997b; Sorimachi *et al.*, 1997). In the Z-repeats, a hydrophobic block of 6–9 residues which is the hallmark of Z-repeats was identified as the binding site (Ohtsuka *et al.*, 1997a). However, we find that repeats zr2–zr3 or zra1–zr4 do not interact in two-hybrid assays. We reason that all Z-repeats should have analogous functions according to their high homology. Therefore, we tested several other binding assays using a recombinant titin Z-repeat fragment zr2–zr3 (amino acids 463–554 in cardiac titin) and the α -actinin fragments R1–R4 and R1–C (amino

Titin– α -actinin interactions in the sarcomeric Z-disk

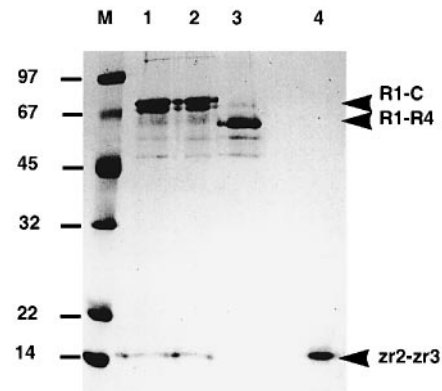


Fig. 5. The central Z-repeats bind to the α -actinin C-terminal domain. The titin Z-repeat fragment zr2–zr3 was assayed in a co-precipitation assay ('pull-down') for binding to the α -actinin rod (R1–R4) and the entire C-terminal region of α -actinin (R1–C). Lane 1, eluate from α -actinin R1–C beads in the absence of Ca^{2+} ; lane 2, eluate from R1–C beads in the presence of 1 mM Ca^{2+} ; lane 3, eluate from R1–R4 beads; lane 4, sample of the input fraction; the ~14 kDa band is the zr2–zr3 fragment. M: marker lane, sizes in kDa. Arrowhead: titin zr2–zr3. Note that the calcium-independent binding is observed only to the R1–C fragment but not to the rod fragment. This indicates that interaction of zr2–zr3 is mediated by the CaM-like C-terminal domain of α -actinin. Some elution of the R1–R4 and R1–C fragments is observed by the denaturing SDS sample buffer as well, probably due to the homodimeric nature of these fragments.

acids 274–746 and 274–894) to establish whether conditions could be found that allow the complex formation *in vitro*.

We could detect interactions between the two-module Z-repeat fragment and α -actinin in the Biosensor and with a bead-based assay, both of which involve immobilization of one component to a hydrophilic matrix. The interactions of the Z-repeat fragment with R1–C resist treatment with up to 4 M urea, and complete regeneration of the Biosensor surface was therefore impossible without loss of binding capacity. This assay was therefore abandoned. The results of the bead-based assay are shown in Figure 5. The α -actinin rod fragment R1–R4 and the entire C-terminal region without the actin-binding domain (R1–C) were coupled to Sepharose beads, and incubated with recombinant zr2–zr3 as described in Materials and methods. The beads were washed, eluted with SDS sample buffer and the eluate analysed by SDS–PAGE. Immobilized zr2–zr3 could be detected from beads coated with R1–C but not with R1–R4 (Figure 5A). Similar results were obtained with the fragment zra1–zr4 (not shown). The central titin Z-repeats therefore interact with α -actinin, and this interaction is dependent on the presence of the C-terminal domain of α -actinin. This interaction also appeared to be independent of the presence of calcium ions (Figure 5). Phospholipids are implicated in the assembly of the Z-disk (Taylor *et al.*, 1997). In our binding assays, the addition of different phospholipids did not alter the titin– α -actinin interaction (data not shown).

Titin, α -actinin and F-actin form ternary complexes *in vitro*

These data suggest that the titin fragments which bind to α -actinin could form a ternary complex with the full-length α -actinin and filamentous actin (F-actin). To test this possibility, we used actin co-sedimentation assays

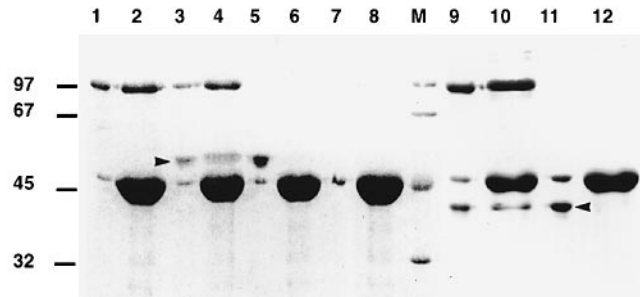


Fig. 6. Titin forms a ternary complex with α -actinin and actin. Mixtures of titin fragments, α -actinin and actin were assayed for their interactions in a co-sedimentation assay. Supernatants and pellets of the co-sedimentation assay were analysed by SDS-PAGE on a 15% gel. The bands of α -actinin (104 kDa) and actin (44 kDa) were found consistently in the pellets. The titin fragments zr4-Z4 and Zq-Z4 were found in the supernatants in the absence of α -actinin. Addition of α -actinin led to co-sedimentation, showing the formation of a ternary complex. Supernatants: lanes 1, 3, 5, 7, 9 and 11. Pellets: lanes 2, 4, 6, 8, 10 and 12. Lanes 1 and 2, α -actinin 2A + actin; lanes 3 and 4, α -actinin 2A + zr4-Z4 + actin; lanes 5 and 6, zr4-Z4 + actin; lanes 7 and 8, actin control; lanes 9 and 10, α -actinin 2A + Zq-Z4 + actin; lanes 11 and 12, Zq-Z4 + actin. M: marker lane, sizes in kDa. Arrowheads: position of the titin fragments.

with the Zq-Z4 fragment as well as with a longer fragment including also the last two Z repeats of titin (zr4-Z4; Figure 1A), in the presence of α -actinin. The α -actinin 2A isoform was used since this isoform was specifically identified as the ligand of titin in the two-hybrid screens, and was obtained as recombinant protein to ensure isoform homogeneity. The results indicate that, under the conditions used, zr4-Z4 co-sedimented with F-actin in the presence of α -actinin, whereas the amount of fragment sedimented was negligible in the absence of α -actinin (Figure 6). The Zq-Z4 fragment co-sedimented to a lower extent (Figure 6). It was not possible to estimate the affinity of the interaction in this assay because at higher concentrations of titin fragments ($>20 \mu\text{M}$), the α -actinin-independent co-sedimentation becomes significant. We tested the influence of different pH conditions and putative modulators [like $\text{Ca}^{2+}/\text{CaM}$ and the phospholipid phosphatidylinositol-4,5-bisphosphate (PIP₂); see Materials and methods] on the binding to actin and α -actinin, but none of these had a significant effect on titin binding.

The N-termini of titin overlap in the central Z-disk region and co-localize with the C-terminus of nebulin

The degree of titin overlap in thick Z-disks is essential for a precise correlation of ultrastructural features to the molecular structure of the Z-disk proteins titin and α -actinin. We therefore refined our mapping data of the titin N-terminus in mammalian slow muscle, using a new antibody against the recombinant N-terminal fragment Z1Z2 in order to achieve higher fixation resistance of the epitope. A modified fixation scheme could now be used that ensured superior preservation of ultrastructural features. The affinity-purified antibody was used on cryosections to determine the epitope position in skeletal muscle Z-disks. We chose *M.longissimus dorsi*, a slow red muscle, for its wide Z-disks and the good preservation of ultrastructure. Low-density labelling was used to avoid obscuring a possible separation of epitopes, and shows specific decoration of sarcomeric Z-disks (Figure 7A and

B). A second marker in the Z-disk, the C-terminal SH3-domain of the actin-filament ruler nebulin (Labeit and Kolmerer, 1995b), decorates Z-disks at a similar position (Figure 7C). The position of gold particles was determined by image analysis of digitized electron microscopy (EM) micrographs, and the histogram obtained fitted a Gaussian distribution. We observe that in the 60–65 nm *longissimus dorsi* Z-disks, the titin Z1Z2 epitope, as monitored by the gold particle distribution, shows two equidistant symmetrical peaks near the edge of the Z-disk, $\sim 30 \pm 10$ nm from the centre (Figure 7D). The two peaks fall within a broad central peak observed at lower resolution in cardiac Z-disks (not shown). Similarly, the nebulin SH3-domain labels 32 ± 12 nm from the Z-disk centre. Together with the previous localization data of the titin Zq-Z4 region at the Z-disk edge (Gautel *et al.*, 1996; Yajima *et al.*, 1996), our refined mapping of the titin N-terminus shows that the region between Zq and the N-terminus is indeed overlapping by ~ 60 – 70 nm in *longissimus dorsi*. This implies that over most of the actin overlap region of the Z-disk, titin molecules from opposite sarcomere halves, which are constructed largely from the titin Z-repeats, run antiparallel.

Discussion

For the assembly of the Z-disk, two mechanisms have to be spatially and temporally coordinated: the capping of actin filaments, presumably by capZ protein (Schafer *et al.*, 1995), and the cross-linking of these overlapping filaments by α -actinin. The molecular ruler proteins of the Z-disk, titin and nebulin/nebulette, are therefore expected to provide in a concerted way specific attachment sites for these proteins as well as for factors possibly involved in the control of capping activity and cross-linking.

In this study, we have identified a novel interaction between titin and α -actinin which involves the formation of a dimerization-independent 1:1 complex with the two central slrs of the rod domain of α -actinin. The two proteins interact with nanomolar dissociation constants in a region of titin which previously has been assigned to the edge of the Z-disk (Gautel *et al.*, 1996; Yajima *et al.*, 1996). This is the first detailed description of the function of α -actinin slrs as protein interaction modules with ligands other than α -actinin itself. The 70 residue titin region has no obvious homology to any proteins other than titin. We suggest that the binding site defined here is distinct from that of other interactions with α -actinin.

Our observation that titin binding is dependent on both the slrs 2 and 3 suggests further that the binding site is formed by both folded three-helix bundles. It seems unlikely that the linker between the repeats is the binding site, as the truncation of slr2 leaves this region intact yet abolishes titin interaction. Furthermore, in agreement with previous studies on the dimerization properties of rod fragments of α -actinin (Kahana and Gratzer, 1991; Flood *et al.*, 1995), we observe no detectable dimer formation of recombinant R2-R3 but strong association with the titin Zq fragment (Figure 4). This supports the notion that the titin-binding site is formed independently on an α -actinin monomer. The 70 residue rod-binding domain of titin is highly conserved between human and chicken, which underlines its evolutionarily conserved function in

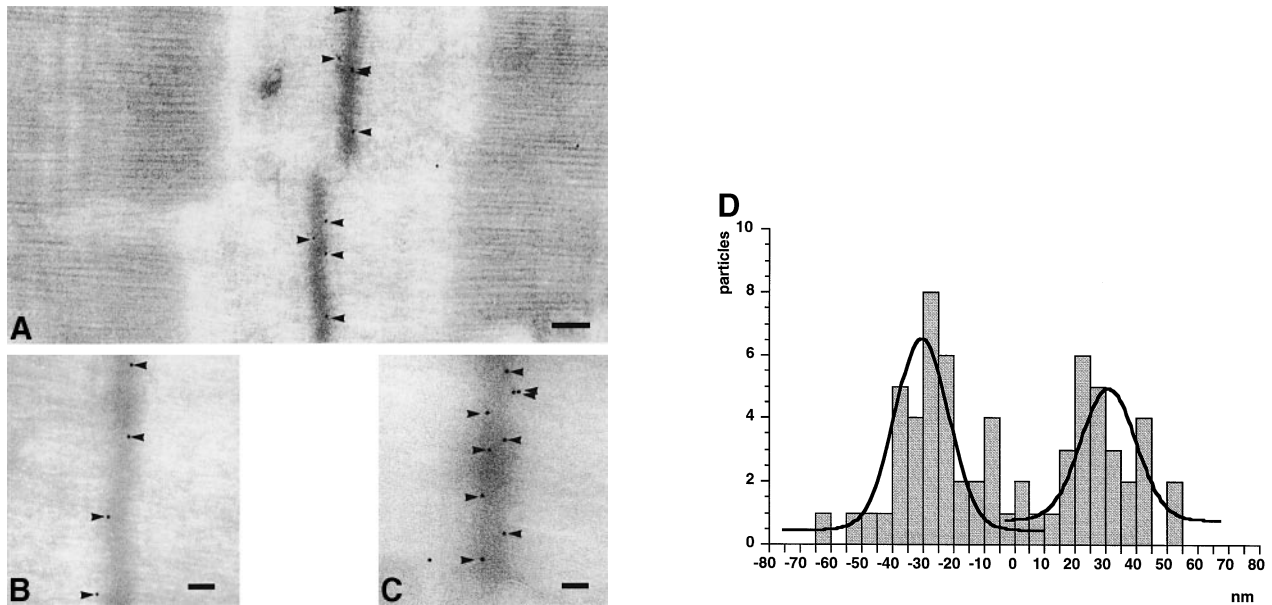


Fig. 7. (A) Immuno-electron microscopy demonstrating the localization of the polyclonal antibody TZ1Z2-ra to Z-disks in rabbit *longissimus dorsi* muscle. Gold particles are found at the Z-disk close to the actin overlap region (arrowheads). Scale bar: 184 nm. (B) Higher magnification shows the label position of titin Z1Z2 at the edge of the actin overlap region (dark region) similar to that of the nebulin SH3 domain labelled by the antibody NSH3-ra (C). Scale bars: 100 nm. (D) Distribution of TZ1Z2-ra gold particles sampled over 24 Z-disks. The distribution of the nanogold particles was analysed as described in Materials and methods. Two centrosymmetrical clusters are observed. Gaussian distributions were fitted to the histograms; the particle distributions show two peaks at ~30 nm on either side of the Z-disk midline (set to 0 nm).

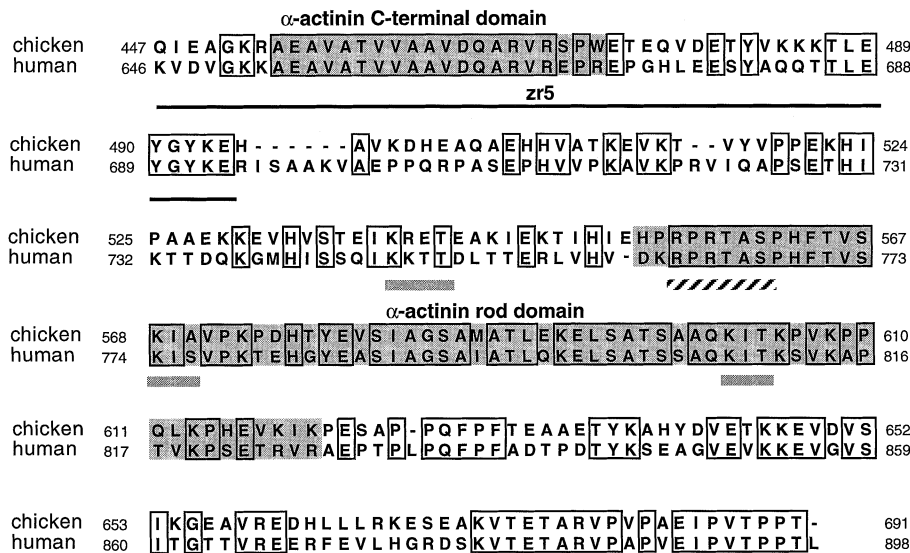


Fig. 8. The two different sorting signals for α -actinin on Z-disk titin. A multiple sequence alignment demonstrates the high cross-species conservation of the two principal sorting signals between chicken titin (DDBJ/EMBL/GenBank accession no. D83390) and human titin (DDBJ/EMBL/GenBank accession no. X90568). The Z-repeat zr5 is shown with the binding site defined by Ohtsuka *et al.* (1997b) shaded in grey. Note the totally conserved cluster of hydrophobic residues which are the hallmark of Z-repeats. This binding site is separated by ~70 residues of poorly conserved sequence from the rod-binding domain in Zq (shaded in grey) which again is highly conserved between chicken and human titin. Putative phosphorylation sites are underlined with bars. Identical residues are boxed.

Z-disk assembly (Figure 8). C-terminal truncation of this motif in the study by Ohtsuka *et al.* (1997b) abolishes the rod interaction. Accordingly, we observe a loss of α -actinin binding when the 70 residue region is truncated N-terminally (Figure 1C). We suggest, therefore, that the conserved 70 residues adopt a specific conformation that is crucial for the formation of the α -actinin-binding site, and which is destroyed by either N- or C-terminal deletions.

Actinin-associated LIM protein (ALP) from muscle was

shown recently to bind to the α -actinin rod (Xia *et al.*, 1997). This binding site overlaps with the titin-binding site on α -actinin. Therefore, those α -actinin molecules not bound to titin would have free binding sites for ALP. Since muscle LIM proteins have been implicated in muscle differentiation and cytoarchitectural organization (Arber *et al.*, 1997; Pomiès *et al.*, 1997), a more direct involvement of the titin- α -actinin-actin complex and additional proteins in the control of myofibrillogenesis is likely. Interestingly, the titin-binding region on α -actinin is also highly

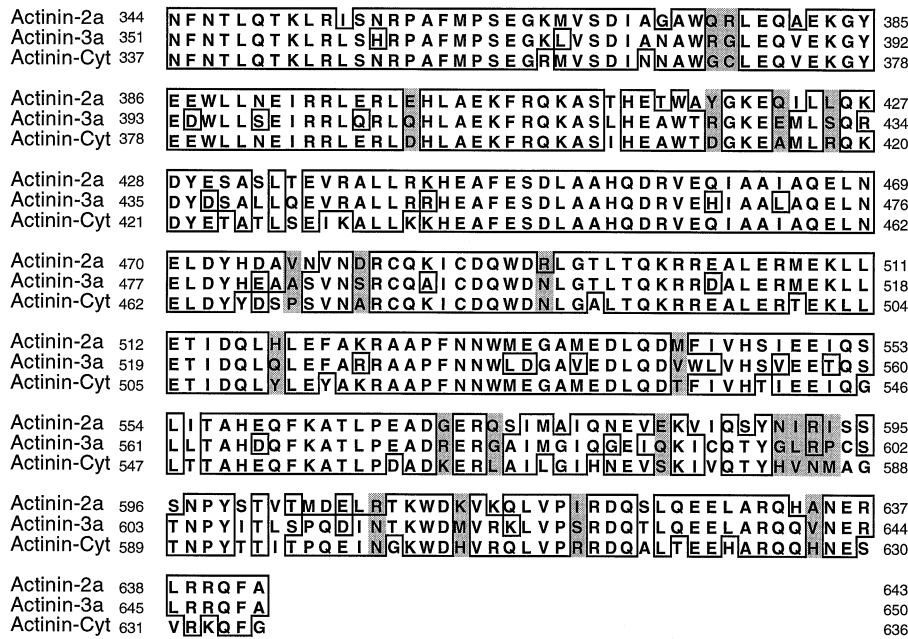


Fig. 9. Comparison of the central spectrin-like repeats of the muscle isoforms of α -actinin 2A and 3A (DDBJ/EMBL/GenBank accession no. M86406 and M86407) and the human placenta isoform (DDBJ/EMBL/GenBank accession no. X15804). Despite a high overall homology, several amino acid exchanges (shaded) discriminate the muscle and non-muscle α -actinins. These residues are possibly involved in titin interaction.

conserved between the cytoplasmic and sarcomeric isoforms (Blanchard *et al.*, 1989) (Figure 9). Despite this high degree of homology, we have not isolated any clones of a non-muscle α -actinin, underlining the specificity of α -actinin isoform sorting to the Z-disk by specific titin interactions.

We have demonstrated previously that the central Z-disk region of titin is constructed in a modular fashion from the 45 residue Z-repeats (Gautel *et al.*, 1996). The highly homologous, invariant repeats (termed zr1 and zr5 in Gautel *et al.*, 1996; Ohtsuka *et al.*, 1997a; Peckham *et al.*, 1997) are separated by between two and five or possibly more repeats in mammals (Gautel *et al.*, 1996; Peckham *et al.*, 1997; Sorimachi *et al.*, 1997). The zig-zag Z-disks with one Z-filament in the avian fast white muscles are assembled from a titin/connectin isoform with only two Z-repeats (Yajima *et al.*, 1996; Ohtsuka *et al.*, 1997a). Mammalian Z-disks with two or more Z-filaments (Rowe, 1973) contain four or more titin Z-repeats (Gautel *et al.*, 1996; Peckham *et al.*, 1997; Sorimachi *et al.*, 1997). It is therefore plausible that the ultrastructural feature of a single Z-filament requires the presence of two titin Z-repeats, orienting two pairs of Z-filaments orthogonally. Two previous studies (Ohtsuka *et al.*, 1997a; Sorimachi *et al.*, 1997) identified the C-terminal Z-repeat, (zr5 according to Gautel *et al.*, 1996; Ohtsuka *et al.*, 1997a) as the major interaction site for the α -actinin C-terminal domain. The binding data on the central type of Z-repeats were conflicting; Ohtsuka *et al.* (1997a) detected no interaction with the chicken zr2 in two-hybrid analysis and, similarly, our studies using nitrocellulose membrane dot-blot (Gautel *et al.*, 1996) or two-hybrid assays could detect no interaction of fragments like zr2–zr3 or zr1–zr4 (Figure 1A). However, using a hydrophilic matrix support, we can now demonstrate that two-module fragments of the central titin Z-repeats show binding to the α -actinin C-terminal domain in a pulldown assay (Figure

5). Possibly, on hydrophobic nitrocellulose supports, the hydrophobic binding site (highlighted in Figure 7) is adsorbed and inaccessible. Interestingly, the highly homologous flanking repeats zr1 and zr5 seem to interact most strongly with α -actinin, and a successive cooperative interaction, starting with the flanking repeats, could therefore explain why the central repeats show different behaviours in some assays. We conclude that the central titin Z-repeats can bind to the α -actinin CaM-like C-terminal domain similarly to the flanking repeats, and hence indeed represent repetitive binding modules expressed in variable copy number (Gautel *et al.*, 1996). Due to the overlap of antiparallel titin molecules interacting with antiparallel α -actinin dimers, it is also conceivable that one strong titin interaction per α -actinin molecule suffices for Z-disk sorting.

The proximity of the α -actinin-binding sites in zr5 and in Zq are highlighted in the sequence comparison in Figure 8. The high degree of conservation of the hydrophobic binding site in zr5 and of the 70 residue region in Zq is evident. The proximity of the two distinct binding sites and the evolutionary homology of the peripheral Z-repeats, zr1 and zr5, (Gautel *et al.*, 1996) suggests that the outermost α -actinin molecules in the Z-disk are sorted differentially from molecules further inside the Z-disk. Interaction sites include the rod domain as well as the two C-terminal domains which could bind to zr5 and zr1 from opposite titin filaments. Since the rod-binding site on titin is present in only one copy per half-sarcomere, the α -actinin molecules nearer the centre of the Z-disk can only interact via their C-terminal domains with the central type of titin Z-repeat.

The unique interaction of titin and α -actinin at the Z-disk edge possibly represents a termination motif for α -actinin incorporation, and perturbation of this mechanism would be expected to result in Z-disk anomalies. This possible function of the α -actinin rod interaction with titin

is supported by the earlier study by Schultheiss *et al.* (1992), where a C-terminally deleted α -actinin was transfected into myogenic cells. Despite the lack of the titin-binding C-terminal domain, this truncated peptide was still targeted to nascent Z-disks. At later stages of myofibrillogenesis, it caused gross enlargement of the Z-disk and ultimately myofibril breakdown. This dominant-negative phenotype might be explained by possible heterodimer formation with endogenous α -actinin. However, our data now offer a molecular explanation at the level of the differential sorting mechanisms of α -actinin molecules to the Z-disk.

The spacing of Z-filaments (α -actinin) in longitudinal projections of Z-disks is ~ 38 nm and thus close to the ~ 36 nm pseudo-repeat of actin in vertebrate thin filaments (Yamaguchi *et al.*, 1985; Luther, 1991). However, the overlap of actin filaments is highly variable, ranging from ~ 10 nm to >100 nm (Yamaguchi *et al.*, 1985; Luther, 1991). Correspondingly, the number of cross-linking Z-filaments ranges between one in non-mammalian fast muscles (Luther, 1991) and 2–4 Z-filaments in mammalian Z-disks (Rowe, 1973). Owing to the three-dimensional lattice formed in the Z-disk, only every second Z-filament is visible in longitudinal sections, whereas the next filament pair is orthogonal to the projection plane (Luther, 1991). The spacing of successive filaments could be determined in the simple Z-disk in fish muscle (Luther, 1991) which contains only one Z-filament in longitudinal projection. The two almost orthogonally oriented pairs are spaced 15–20 nm apart. In the reconstructions of the more complex mammalian Z-disks by Schroeter *et al.* (1996), orthogonal Z-filaments are spaced 16 ± 9 nm and planar filaments 28 ± 9 nm apart. In nemaline rods, which are presumably binary complexes of actin and α -actinin, the spacing is ~ 19 nm (Morris and Squire, 1990). Allowing for the standard deviation of these measurements, pairs of Z-filaments are therefore placed at angles of 80 – 90° approximately every 17–18 nm. Within the high variability of the F-actin helical twist (Egelman *et al.*, 1982), this is about a quarter turn of the F-actin long-pitch helix for each Z-filament (Luther, 1991).

Since orthogonally arranged pairs of Z-filaments are spaced by ~ 15 – 20 nm (Luther, 1991; Schroeter *et al.*, 1996), the interactions of titin Z-repeats and successive pairs of α -actinin molecules must roughly allow for this spacing. Also, as pointed out by Luther (1991), the arrangement of the Z-disk must to some degree follow the helical structure of the actin filaments with a variable half-repeat spacing of between 35 and 38 nm (Egelman *et al.*, 1982). Single titin Z-repeats are ~ 45 residues in length (Gautel *et al.*, 1996). Depending on their secondary structure in the complex with the CaM-like domain of α -actinin, they could span a length of up to 17 nm in a largely β conformation or as extended sequence (based on the $\text{C}\alpha$ -distances of ~ 3.8 nm for β strands). This length is in good agreement with the orthogonal spacing of Z-filaments in both mammalian and non-mammalian Z-disks. Since all Z-repeats appear to be involved in α -actinin binding, the successive arrangement of α -actinin molecules into Z-filaments can be explained readily by successive pairs of titin-binding sites spaced ~ 17 nm apart. Clearly, the complex structures of the two titin- α -actinin

interactions are now needed for a more detailed understanding of the sorting mechanism.

The interactions of titin with α -actinin, involving both the rod and the C-terminal domain at the Z-disk edge, enforce a special path for titin molecules entering the Z-disk. Since the α -actinin rod measures ~ 23 nm in length (Flood *et al.*, 1995), and titin binds in the middle of the rod, the titin molecule should run for ~ 10 nm along the α -actinin rod. The next interaction site is localized in zr5, where titin will bind to the C-terminal domain of α -actinin (Figure 8). At this point, the titin molecule must change the orientation of its path to be linked to the successive α -actinin molecules which could now interact with the Z-repeats. It must therefore run parallel to the actin filaments in the Z-repeat region. Our ultrastructural analysis could now place the position of the N-terminal domains of titin at the edge of the actin overlap region, with molecules entering from two sarcomere halves crossing over the Z-disk centre by ~ 30 nm (Figure 7). Therefore, only at each Z-disk edge will α -actinin molecules be bound by two overlapping, antiparallel titin molecules by the interaction of their rod domains as well as their CaM-like domains. This special pair of α -actinin molecules will be anchored to the two essentially identical high-affinity sites in Z-repeats zr1 and zr5. The two C-terminal domains could interact in the same fashion with the antiparallel Z-repeats, similarly to the two actin-binding domains that interact with antiparallel actin filaments.

Our biochemical and ultrastructural observations can be summarized in a molecular model for the layout of titin, actin and α -actinin in the central Z-disk as depicted in Figure 10. The region C-terminal from Z4 may be complexed with F-actin by additional proteins or by direct interactions, e.g. between Z10 and I1 (Linke *et al.*, 1997). Titin can enter the Z-disk essentially via two similar paths. Both paths are defined by the constraints imposed by the protein interactions with α -actinin, the ultrastructural position of the N-terminus (Figure 7) and that of Zq and of Z4 immediately at the outer edge of the central Z-disk (Gautel *et al.*, 1996; Yajima *et al.*, 1996). In both cases, titin must run along the outmost α -actinin molecule for at least the length of half the rod domain to bridge the adjacent binding sites in Zq and zr5. The maximal number of Z-filaments predicted by this model would be the highest integer of half the number of Z-repeats. This is in excellent agreement with observations on thick Z-disks that show 3–4 Z-filaments (Rowe, 1973; Yamaguchi *et al.*, 1985) with up to seven Z-repeats, and fast skeletal muscle fibres with four Z-repeats (Ohtsuka *et al.*, 1997a; Peckham *et al.*, 1997) that show two Z-filaments (Rowe, 1973). The chicken *M. pectoralis* Z-disk represents a minimal version with only two Z-repeats and one Z-filament (see above). An alternative path of titin involving a crossing-over to an antiparallel actin filament would provide a greater cross-linking of the entire structure but seems less likely for reasons of symmetry. The most plausible path in Figure 10 places the titin N-terminus close to the barbed end of the parallel thin filament, and the previously defined regulatory phosphorylation sites in the proline-rich insertion between Z2 and Z3 (Gautel *et al.*, 1996) could therefore be involved in the control of thin filament capping. This concept is supported by our observation of the position of the regulatory SH3 domain of nebulin,

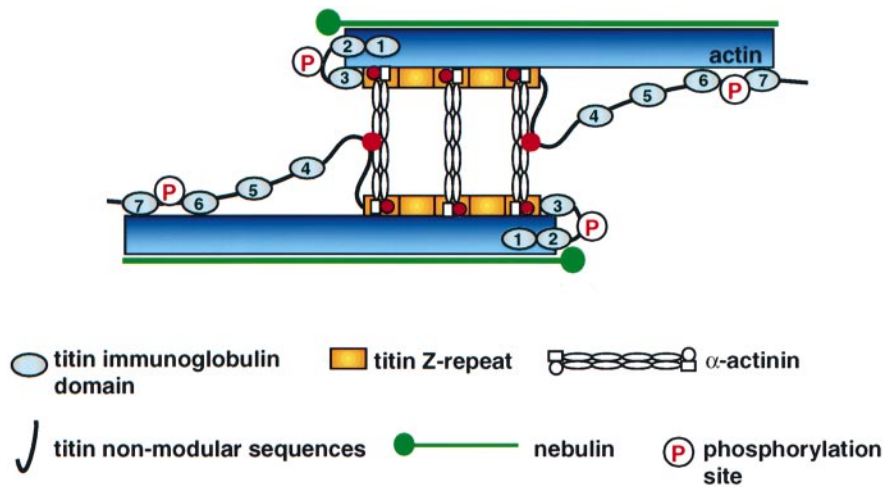


Fig. 10. Molecular structure of the sarcomeric Z-disk. The most likely path of titin into the Z-disk runs parallel to the thin filament for most of its length. Established protein interaction sites are highlighted in red. Titin domains are numbered according to Labeit and Kolmerer (1995a). Along the outermost pair of α -actinin molecules, titin is linked to the α -actinin rod and to the CaM-like domain. In the central Z-disk, titin Z-repeats (golden squares) coordinate successive α -actinin molecules. The nebulin SH3 domain (green circle) and the proline-rich N-terminus of titin are in close proximity and could interact; proteins binding to Z1Z2 or Z3 of titin or to the C-terminal region of nebulin could be involved in the control of barbed-end capping. The position of regulatory SP-rich phosphorylation sites (Gautel *et al.*, 1996) is shown. Only every second α -actinin molecule is shown in the central Z-disk, as they would appear in longitudinal sections of the lattice. Since the spacing of thin filaments and concomitantly the angle of the Z-filaments is variable (Yamaguchi *et al.*, 1985), the α -actinin links are shown schematically at right angles. The position of the titin N-terminus is arbitrarily shown with some flexibility in the linker segment.

which localizes close to the titin N-terminus (Figure 7). This co-localization would allow the previously proposed interaction of proline-rich sequences in titin and the nebulin SH3 domain (Gautel *et al.*, 1996; Politou *et al.*, 1997). Future reconstructions of the α -actinin–titin complex might allow one to define these interactions in structural detail and thus to elucidate the molecular basis of Z-disk assembly.

Materials and methods

Yeast two-hybrid screens and two-hybrid protein interaction analysis

A region of titin comprising residues 695–990 of human cardiac titin was cloned into the pLexA vector (Stenmark *et al.*, 1995). The plasmid was transformed into the *Saccharomyces cerevisiae* L40 reporter strain using a modified lithium acetate protocol (Vojtek *et al.*, 1993). The bait-bearing strain subsequently was co-transformed with a human skeletal muscle cDNA library in the pGAD-10 Gal4 activation domain vector (Clontech). Selection for *HIS3* reporter gene activation was performed on selection agar plates without histidine, leucine and tryptophan (SD-LWH), essentially as described (Stenmark *et al.*, 1995). Colonies appearing after 4–5 days at 30°C were assayed in filter assays for β -galactosidase activity, and library plasmids from positive clones were isolated following the Matchmaker protocol (Clontech) and their inserts sequenced. In confirming and mapping the interaction between titin and α -actinin, constructs encoding various regions of both proteins were cloned into pLexA and pGAD-10 vectors, respectively, and then co-transformed into L40 cells. Growth on SD-LWH plates as well as β -galactosidase activity were then assayed. Triplicate liquid β -galactosidase assays with *o*-nitrophenol- β -D-galactopyranoside as substrate were carried out from separate transformants using a modified version of the Matchmaker protocol (Clontech). The units are relative and not directly comparable with other publications. Some pLexA titin constructs alone activated the *HIS3* and β -galactosidase reporter genes ($\Delta 1$, $\Delta 2$, $\Delta 3$ and $\Delta 4$ constructs). Addition of 5 or 10 mM 3-aminotriazole (Sigma) was used to suppress background growth of these transformants on SD-LWH plates. β -Galactosidase activities measured when these constructs were co-transformed with pGAD-10 α -actinin constructs were corrected by subtraction of the values obtained upon co-transformation with a pGAD construct shown not to interact with titin. The expression of the fusion constructs was monitored in transformed L40 cells by

Western blotting with a monoclonal anti-lexA antibody (Clontech) and confirmed the presence of correctly sized fusion proteins.

For analysis of the interactions of Z-repeats, the repeats zr2–zr3 (amino acids 463–554), zra1–zr4 (amino acids 550–644) and the fragments Z1–zr3 (amino acids 1–554) were also cloned into pLexA (Figure 1A).

cDNA cloning and sequencing

Titin and α -actinin cDNA constructs for two-hybrid analysis were amplified from total human cardiac DNA (Clontech) by PCR (Saiki *et al.*, 1985). Primer design was based on the human cardiac titin sequence (DDBJ/EMBL/GenBank accession no. X90568) and the human skeletal muscle α -actinin 2 sequence (DDBJ/EMBL/GenBank accession no. M86406). Domain nomenclature for titin is as described in Labeit and Kolmerer (1995a) and Gautel *et al.* (1996). Phasing of domains for α -actinin constructs was as determined for chicken cytoskeletal α -actinin (Gilmore *et al.*, 1994). All cloning procedures followed standard protocols (Ausubel *et al.*, 1987). The identity of the derived constructs was verified by DNA sequencing.

Protein expression and purification

Titin and α -actinin cDNA constructs were amplified as described above and cloned into a modified pET vector described previously in Labeit *et al.* (1992). Expression of soluble His₆-tagged polypeptides was then induced in *E. coli* BL21[DE3] using 0.2 mM isopropyl- β -D-thiogalactopyranoside (IPTG). Initial purification was carried out on an Ni-NTA agarose column (Qiagen). Further purification was by ion exchange on a MonoQ column (Pharmacia). Purified proteins were analysed by SDS-PAGE as described (Laemmli, 1970). Full-length α -actinin was expressed with an N-terminally fused His₆ tag and the recognition site for TEV protease (Parks *et al.*, 1994). After standard Ni-NTA affinity chromatography, the tag was cleaved off by recombinant TEV protease (Gibco-BRL, UK) and removed by ion exchange chromatography on a MonoQ column, leaving the recombinant protein with additional N-terminal sequence Gly–Ser–Ser.

Co-precipitation assays

The recombinant α -actinin fragments R1–R4 (residues 274–746) and R1–C (274–894) were coupled to CH-activated Sepharose beads (Pharmacia) following the manufacturer's instructions at a density of ~1 mg/ml beads. Beads were subsequently blocked with ethanolamine and then 10 mg/ml bovine serum albumin (BSA). The purified titin fragment zr2–zr3 was incubated for 10 min at 25°C in binding buffer [20 mM HEPES pH 7, 100 mM NaCl, 1 mM dithiothreitol (DTT), 0.1% Triton X-100] at a protein concentration of 5 μ M with 50 μ l of coated Sepharose beads

in 100 μ l volumes of assay buffer. In some assays, calcium chloride (1 mM), or 0.1 mg/ml phosphatidylserine, phosphatidylethanolamine or PIP₂ (the latter three as micellar solutions in 0.1% Triton X-100) were added. Control beads were the ones coated with the α -actinin rod alone. Beads were separated from the supernatant by centrifugation in a perforated reaction tube, and washed three times with 0.5 ml of binding buffer. Specifically bound protein was eluted twice with 30 μ l of 4 \times sample buffer at 95°C, the fractions pooled and 15 μ l aliquots were analysed on 15% SDS-PAGE gels (Laemmli, 1970).

Biosensor assays

The α -actinin rod domain R1–R4 was coupled to carboxymethyl dextrane (CMD)-coated biosensor cuvettes (Affinity, Germany) following the manufacturer's instructions. Briefly, CMD cuvettes were activated by EDC/NHS and α -actinin R1–R4 was coupled at 0.1 mg/ml in 10 mM sodium acetate, pH 6. Protein densities of \sim 1000 arcsec units were aimed at to prevent steric inhibition. Protein interactions with titin Zq–Z4 were monitored on an IAsys Auto+ biosensor (Affinity) in binding buffer with sampling rates of 0.3/s. The titin Zq–Z4 concentrations were between 0.1 and 50 μ M. Regeneration of the sensor cuvette was achieved with 0.5 M ethanolamine pH 8 or 1 M NaCl. The observed binding curves could be well fitted assuming single-phase kinetics ($R^2 \sim 0.98$), and single-phase association rates accordingly were calculated from the fits using the FastFit software (Affinity, Germany). Linear plots of the association rates versus ligand concentrations could be fitted to the data with a correlation coefficient of 0.98 and yielded k_{on} and k_{off} values.

Chemical cross-linking

Cross-linking was performed using the amino group-reactive cross-linker Bis(sulfosuccinimidyl)suberate (Pierce Chemical Co) at 1.7 mM for 1 h on ice. The expressed recombinant polypeptides R1–R4, Zq–Z4 and R2–R3 were used at approximately equimolar concentrations of 12.6 μ M (R1–R4), 6.3 μ M (R2–R3) and 12.5 μ M (Zq–Z4) in 20 mM HEPES pH 7, 50 mM NaCl, 1 mM EDTA. Cross-linked protein was visualized by SDS-PAGE on a 12% gel (Laemmli, 1970).

Actin co-sedimentation assay

Actin co-sedimentation assays were carried out essentially as described (Way *et al.*, 1992). Briefly, 20 μ M F-actin was mixed with 5 μ M α -actinin and different titin fragments in 10 mM Tris, pH 8.0 (or pH 7.0), 100 mM (or 25 mM) NaCl, 1 mM MgCl₂, 1 mM EDTA, 0.1 mM ATP and 0.1 mM DTT, and incubated at room temperature for 30 min. Then 5 μ M Zr4–Z4, Zq–Z4, zr2–zr3 or zra1–zr4, α -actinin or mixtures of these were added. In some assays, 10 μ M CaM, 1 mM CaCl₂ or 50 μ M PIP₂ in 0.1% Triton X-100 were added. Polymerized actin was separated by ultracentrifugation in a Beckman airfuge for 30 min at 28 p.s.i. Pellets and supernatants were brought to the same total volume of SDS sample buffer, boiled, and equal volumes were loaded on 15% SDS-polyacrylamide gels. BSA was used as a control for unspecific trapping; no significant trapping was observed.

Antibodies, immunoelectron microscopy and image analysis

A polyclonal serum against the recombinant N-terminal titin fragment Z1Z2 (Gautel *et al.*, 1996) was raised in rabbits using a standard immunization protocol. The antigen was coupled to NHS-hitrap columns (Pharmacia) following the manufacturer's instructions and specific antibody affinity-purified as described (Harlow and Lane, 1988). The antibody NSH3-ra was raised against the recombinant SH3 domain of nebulin (HSRNANE, DDBJ/EMBL/GenBank accession no. X83957; residues 6604–6669).

Rabbit *longissimus dorsi* muscle was excised immediately post-mortem from a freshly killed New Zealand White rabbit, dissected in ice-cold rigor solution and small fibre bundles were mounted on wooden supports. Fibres were fixed in 4% paraformaldehyde rigor buffer (pH 6.8), at room temperature for 2 h. Fibres intended for cryosectioning were dissected later from the main bundle under fixative, rinsed once in rigor buffer and cryoprotected by infiltrating with sucrose 2.1 M (3 \times 10 min), mounted on a small Cu block and frozen in liquid nitrogen. Thin sections 50–100 nm thick were cut and mounted on Cu/Pd formvar-coated grids, blocked against non-specific binding with 10% fetal calf serum (FCS) in phosphate-buffered saline (PBS) for 30 min and labelled with the primary antibody (1:30 in 5% FCS), followed by protein A gold (10 nm). After six successive washes in PBS, grids were floated on drops of 1% glutaraldehyde for 5 min, rinsed in water (4 \times 5 min), and later stained with 0.3% uranyl acetate as described in Lakey *et al.* (1990). Grids were viewed on a Philips 400T electron microscope at 80 kV. EM negatives were scanned at 400 d.p.i. using a Linotype Sapphire scanner. Six EM

negatives and a total of 24 Z-disks were analysed. Z-disks were aligned vertically and gold particle positions determined using the particle analysis software in NIH-Image. In the case of NSH3-ra, 12 Z-disks were analysed. The derived X-positions were normalized to the Z-disk centre and calibrated to nm distances using the A-band length (1.58 μ m) as internal length standard. The particle positions were plotted as histograms using Kaleidagraph (Abelbeck software), and Gaussian distributions were fitted using the same software.

Acknowledgements

We are greatly indebted to Matti Saraste for his generous support and to Kevin Leonard for his critical help with the EM work and image analysis. We thank Belinda Bullard for fruitful discussions and critical comments on the manuscript. Gunter Stier provided essential help in TEV cleavage of fusion proteins. This work was supported by the Deutsche Forschungsgemeinschaft (Ga405/3-1) and the DLR (GR1-104-97).

References

- Arber,S., Hunter,J., Ross,J., Hongo,M., Sansig,G., Borg,J., Perriard,J.-C., Chien,K. and Caroni,P. (1997) MLP-deficient mice exhibit a disruption of cardiac cytoarchitectural organization, dilated cardiomyopathy, and heart failure. *Cell*, **88**, 393–403.
- Ausubel,F.M., Brent,R., Kingston,R.E., Moore,D.D., Seidman,J.G., Smith,J.A. and Struhl,K. (1987) *Current Protocols in Molecular Biology*. J.Wiley and Sons, Inc., New York.
- Beggs,A.H., Byers,T.J., Knoll,J.H., Boyce,F.M., Bruns,G.A. and Kunkel,L.M. (1992) Cloning and characterization of two human skeletal muscle alpha-actinin genes located on chromosomes 1 and 11. *J. Biol. Chem.*, **267**, 9281–9288.
- Blanchard,A., Ohanian,V. and Critchley,D. (1989) The structure and function of alpha-actinin. *J. Muscle Res. Cell Motil.*, **10**, 280–289.
- Dabiri,G.A., Turnacioglu,K.K., Sanger,J.M. and Sanger,J.W. (1997) Myofibrillogenesis visualized in living embryonic cardiomyocytes. *Proc. Natl Acad. Sci. USA*, **94**, 9493–9498.
- Davies,R.J. and Pollard Knight,D. (1993) An optical biosensor system for molecular interaction studies. *Am. Biotechnol. Lab.*, **11**, 52–54.
- Dlugosz,A.A., Antin,P.B., Nachmias,V.T. and Holtzer,H. (1984) The relationship between stress fiber-like structures and nascent myofibrils in cultured cardiac myocytes. *J. Cell Biol.*, **99**, 2268–2278.
- Egelman,E.H., Francis,N. and DeRosier,D.J. (1982) F-actin is a helix with a random variable twist. *Nature*, **298**, 131–135.
- Flood,G., Kahana,E., Gilmore,A.P., Rowe,A.J., Gratzner,W.B. and Critchley,D.R. (1995) Association of structural repeats in the alpha-actinin rod domain. *J. Mol. Biol.*, **252**, 227–234.
- Fürst,D.O., Osborn,M., Nave,R. and Weber,K. (1988) The organization of titin filaments in the half-sarcomere revealed by monoclonal antibodies in immunoelectron microscopy; a map of ten non-repetitive epitopes starting at the Z line extends close to the M line. *J. Cell Biol.*, **106**, 1563–1572.
- Fürst,D.O., Osborn,M. and Weber,K. (1989) Myogenesis in the mouse embryo: differential onset of expression of myogenic proteins and the involvement of titin in myofibril assembly. *J. Cell Biol.*, **109**, 517–527.
- Gautel,M., Goulding,D., Bullard,B., Weber,K. and Fürst,D.O. (1996) The central Z-disk region of titin is assembled from a novel repeat in variable copy numbers. *J. Cell Sci.*, **109**, 2747–2754.
- Gilmore,A.P., Parr,T., Patel,B., Gratzner,W.B. and Critchley,D.R. (1994) Analysis of the phasing of four spectrin-like repeats in alpha-actinin. *Eur. J. Biochem.*, **225**, 235–242.
- Harlow,E. and Lane,D. (1988) *Antibodies: A Laboratory Manual*. Cold Spring Harbor Laboratory Press, Cold Spring Harbor, NY.
- Jeng,C.J. and Wang,S.M. (1992) Interaction between titin and α -actinin. *Biomed. Res.*, **13**, 197–202.
- Kahana,E. and Gratzner,W.B. (1991) Properties of the spectrin-like structural element of smooth-muscle α -actinin. *Cell Motil. Cytoskel.*, **20**, 242–248.
- Labeit,S. and Kolmerer,B. (1995a) Titins: giant proteins in charge of muscle ultrastructure and elasticity. *Science*, **270**, 293–296.
- Labeit,S. and Kolmerer,B. (1995b) The complete primary structure of human nebulin and its correlation to muscle structure. *J. Mol. Biol.*, **248**, 308–315.
- Labeit,S., Gautel,M., Lakey,A. and Trinick,J. (1992) Towards a molecular understanding of titin. *EMBO J.*, **11**, 1711–1716.

- Laemmli, U.K. (1970) Cleavage of structural proteins during the assembly of the head of bacteriophage T4. *Nature*, **227**, 680–685.
- Lakey, A., Ferguson, C., Labeit, S., Reedy, M., Larkins, A., Butcher, G., Leonard, K. and Bullard, B. (1990) Identification and localization of high molecular weight proteins in insect flight and leg muscle. *EMBO J.*, **9**, 3459–3467.
- Linke, W.A., Ivemeyer, M., Labeit, S., Hinssen, H., Ruegg, J.C. and Gautel, M. (1997) Actin–titin interaction in cardiac myofibrils: probing a physiological role. *Biophys. J.*, **73**, 905–919.
- Luther, P.K. (1991) Three-dimensional reconstruction of a simple Z-band in fish muscle. *J. Cell Biol.*, **113**, 1043–1055.
- Maruyama, K. (1997) Connectin/titin, giant elastic protein of muscle. *FASEB J.*, **11**, 341–345.
- Maruyama, K., Matsubara, S., Natori, R., Nonomura, Y., Kimura, S., Ohashi, K., Murakami, F., Handa, S. and Eguchi, G. (1977) Connectin, an elastic protein of muscle: characterization and function. *J. Biochem.*, **82**, 317–337.
- Morris, E.P. and Squire, J.M. (1990) The three-dimensional structure of the nemaline rod Z-band. *J. Cell Biol.*, **111**, 2961–2978.
- Ohtsuka, H., Yajami, H., Maruyama, K. and Kimura, S. (1997a) The N-terminal Z repeat 5 of connectin/titin binds to the C-terminal region of α -actinin. *Biochem. Biophys. Res. Commun.*, **235**, 1–3.
- Ohtsuka, H., Yajima, H., Maruyama, K. and Kimura, S. (1997b) Binding of the N-terminal 63 kDa portion of connectin/titin to alpha actinin. *FEBS Lett.*, **401**, 65–67.
- Parks, T., Leuther, K., Howard, E., Johnston, S. and Dougherty, W. (1994) Release of proteins and peptides from fusion proteins using a recombinant plant virus proteinase. *Anal. Biochem.*, **216**, 413–417.
- Peckham, M., Young, P. and Gautel, M. (1997) Constitutive and variable regions of Z-disk titin/connectin in myofibril formation: a dominant-negative screen. *Cell Struct. Funct.*, **22**, 95–101.
- Politou, A., Millevoi, S., Gautel, M., Kolmerer, B. and Pastore, A. (1998) SH3 in muscle: solution structure of the nebulin SH3. *J. Mol. Biol.*, in press
- Pomès, P., Louis, H. and Beckerle, M. (1997) CRP1, a LIM domain protein implicated in muscle differentiation, interacts with α -actinin. *J. Cell Biol.*, **139**, 157–168.
- Rowe, R.W.D. (1973) The ultrastructure of the Z discs from white, intermediate and red fibres of mammalian striated muscle. *J. Cell Biol.*, **57**, 261–277.
- Saiki, R.K., Scharf, S., Faloona, F., Mullis, K.B., Horn, G.T., Erlich, H.A. and Arnheim, N. (1985) Enzymatic amplification of beta-globin genomic sequences and restriction site analysis for diagnosis of sickle cell anemia. *Science*, **230**, 1350–1354.
- Schafer, D.A., Hug, C. and Cooper, J.A. (1995) Inhibition of CapZ during myofibrillogenesis alters assembly of actin filaments. *J. Cell Biol.*, **128**, 61–70.
- Schroeter, J.P., Breaudiere, J.P., Sass, R.L. and Goldstein, M.A. (1996) Three-dimensional structure of the Z band in a normal mammalian skeletal muscle. *J. Cell Biol.*, **133**, 571–583.
- Schultheiss, T., Choi, J., Lin, Z.X., DiLullo, C., Cohen-Gould, L., Fischman, D. and Holtzer, H. (1992) A sarcomeric α -actinin truncated at the carboxyl end induces the breakdown of stress fibers in PtK2 cells and the formation of nemaline-like bodies and breakdown of myofibrils in myotubes. *Proc. Natl Acad. Sci. USA*, **89**, 9282–9286.
- Sorimachi, H. *et al.* (1997) Tissue-specific expression and alpha-actinin binding properties of the Z-disc titin: implications for the nature of vertebrate Z-discs. *J. Mol. Biol.*, **270**, 688–695.
- Squire, J. (1981) *The Structural Basis of Muscular Contraction*. Plenum Press, New York.
- Stenmark, H., Vitale, G., Ullrich, O. and Zerial, M. (1995) Rabaptin-5 is a direct effector of the small GTPase Rab5 in endocytic membrane fusion. *Cell*, **83**, 423–432.
- Taylor, R.G., Papa, I., Astier, C., Ventre, F., Benyamin, Y. and Ouali, A. (1997) Fish muscle cytoskeleton integrity is not dependent on intact thin filaments. *J. Muscle Res. Cell Motil.*, **18**, 285–294.
- Tokuyasu, K.T. and Maher, P.A. (1987) Immunocytochemical studies of cardiac myofibrillogenesis in early chick embryos. I. Presence of immunofluorescent titin spots in premyofibril stages. *J. Cell Biol.*, **105**, 2781–2793.
- Trinick, J. (1994) Titin and nebulin: protein rulers in muscle? *Trends Biochem. Sci.*, **19**, 405–409.
- Trinick, J. (1996) Titin as a scaffold and spring. *Curr. Biol.*, **6**, 258–260.
- Turnacioglu, K.K., Mittal, B., Sanger, J.M. and Sanger, J.W. (1996) Partial characterization of zeugmatin indicates that it is part of the Z-band region of titin. *Cell. Motil. Cytoskel.*, **34**, 108–121.
- Vigoreaux, J.O. (1994) The muscle Z band: lessons in stress management. *J. Muscle Res. Cell Motil.*, **15**, 237–255.
- Vojtek, A.B., Hollenberg, S.M. and Cooper, J.A. (1993) Mammalian Ras interacts directly with the serine/threonine kinase Raf. *Cell*, **74**, 205–214.
- Wang, K., McClure, J. and Tu, A. (1979) Titin: major myofibrillar components of striated muscle. *Proc. Natl Acad. Sci. USA*, **76**, 3698–3702.
- Wang, K., Knipfer, M., Huang, Q., van Heerden, A., Hsu, L., Gutierrez, G., Quia, X. and Stedman, H. (1996) Human skeletal muscle nebulin sequence encodes a blueprint for thin filament architecture: sequence motifs and affinity profiles of tandem repeats and terminal SH3. *J. Biol. Chem.*, **271**, 4303–4314.
- Way, M., Pope, B. and Weeds, A.G. (1992) Evidence for functional homology in the F-actin binding domains of gelsolin and α -actinin: implication for the requirements of severing and capping. *J. Cell Biol.*, **119**, 835–842.
- Xia, H., Winokur, S.T., Kuo, W.-L., Altherr, M. and Bredt, D. (1997) Actinin-associated LIM-protein: identification of a domain interaction between PDZ and spectrin-like motifs. *J. Cell Biol.*, **139**, 507–515.
- Yajima, H., Ohtsuka, H., Kawamura, Y., Kume, H., Murayama, T., Abe, H., Kimura, S. and Maruyama, K. (1996) A 11.5-kb 5'-terminal cDNA sequence of chicken breast muscle connectin/titin reveals its Z line binding region. *Biochem. Biophys. Res. Commun.*, **223**, 160–164.
- Yamaguchi, M., Izumimoto, M., Robson, R.M. and Stromer, M.H. (1985) Fine structure of wide and narrow vertebrate muscle Z-lines. *J. Mol. Biol.*, **184**, 621–643.
- Yan, Y., Winograd, E., Viel, A., Cronin, T., Harrison, S.C. and Barnton, D. (1993) Crystal structure of the repetitive segments of spectrin. *Science*, **262**, 2027–2030.

Received July 21, 1997; revised December 17, 1997;
accepted January 12, 1998